

Article

Type and Sources of Salt Efflorescence in Painted Stone Carvings from Pujiang Museum, Sichuan, China

Quanshuai Song ¹, Jianrui Zha ¹, Yulong Bai ², Long Chen ³, Yao Zhang ^{1,4} and Hong Guo ^{1,*}

¹ Institute for Cultural Heritage and History of Science & Technology, University of Science and Technology Beijing, Beijing 100083, China

² Chengdu Institute of Cultural Relics and Archaeology, Chengdu 610072, China

³ Pujiang Museum, Pujiang 611630, China

⁴ Beijing Guowenyan Conservation and Development of Cultural Heritage Co., Ltd., Beijing 100192, China

* Correspondence: guohong@ustb.edu.cn; Tel.: +86-13391852600

Abstract: Painted stone carvings from Pujiang Museum in Chengdu were excavated from the Ming tombs near to Chengdu Metro Line 7. The Ming burial sites were the eunuch graves of the Shu King, and their tomb was constructed mostly of stone and decorated with paintings and carvings on its surface, which are of great value. However, during their burial, these painted stone carvings suffered significant salt damage. In this research, we performed optical microscope (OM) analysis, Raman spectra (RAM), ion chromatography (IC) analysis, X-ray fluorescence spectroscopy (XRF), X-ray powder diffraction (XRD), and petrographic microscopy (PM) to clarify the salt composition and influence. According to the results, the majority of the salt on the painted layer is $\text{CaSO}_4 \cdot 2\text{H}_2\text{O}$. Before excavation, interaction between acid rain, soil, and groundwater created salt efflorescence on the paint layer's surface. The deterioration of the paint layer caused by gypsum was divided into two stages: before excavation and during in situ preservation. This research provides a foundation for the removal and prevention of salt efflorescence.

Keywords: Ming dynasty tombs; gypsum; sources of salt efflorescence



Citation: Song, Q.; Zha, J.; Bai, Y.; Chen, L.; Zhang, Y.; Guo, H. Type and Sources of Salt Efflorescence in Painted Stone Carvings from Pujiang Museum, Sichuan, China. *Crystals* **2023**, *13*, 273. <https://doi.org/10.3390/cryst13020273>

Academic Editor: Carlos Rodriguez-Navarro

Received: 31 December 2022

Revised: 1 February 2023

Accepted: 1 February 2023

Published: 4 February 2023



Copyright: © 2023 by the authors. Licensee MDPI, Basel, Switzerland. This article is an open access article distributed under the terms and conditions of the Creative Commons Attribution (CC BY) license (<https://creativecommons.org/licenses/by/4.0/>).

1. Introduction

Painted stone carving is a specialized form of painting, which refers to the process of painting intricate designs and patterns onto carved stone substrates. This process is similar to the technique used to create murals. Existing painted stone carvings in China can be abundantly found in grottoes, temples, or other religious places [1,2]. A few excavated Buddha statues [3,4] and painted stone carvings have been discovered in burials.

Painted cultural relics are often affected by their materials, processes, and external preservation environment [5]. These factors can induce a variety of diseases, including paint loss, punctate loss, salt damage, and cracks. One of the most significant types of infection is salt damage, which includes salt efflorescence and disruption. The deterioration is difficult to eliminate, can have an irreversible effect on painted cultural relics, and is also known as the 'cancer' of murals [6]. Current research on salt damage in the field of heritage conservation focuses on three points [7]. Firstly, the types and sources of salt. Secondly, the mechanism of efflorescence formation and salt damage generation. Thirdly, the desalination and cleaning methods. In terms of the types, sources, and weathering mechanisms of salt, Guo Hong et al. demonstrated that NaCl and Na_2SO_4 are the most abundant soluble salts in the murals at Dunhuang Mogao Grottoes. The dissolution and recrystallization of NaCl and Na_2SO_4 under the effect of variations in temperature and humidity are the primary factors of crystalline salt damage to murals [8–10]. Luigi Dei used differential thermal analysis to obtain accurate quantitative measurements of mixed salts, such as nitrate, oxalate, and sulphate [11]. Robert J. Flatt quantified the crystallization pressure of sodium sulfate phases by thermodynamic methods to be 10–20 MPa, which is significantly higher than the tensile

strength of natural stones [12]. Heiner Siedel analyzed weathering samples from buildings and monuments in Saxony (Germany) by XRD. Gypsum, magnesium sulphate, and sodium sulphate were the most abundant salts. The high frequency of sulphates results from the long-term effects of air pollution [13]. Liu et al. analyzed sandstone samples from the Yungang Grottoes by XRD and EDAX (Energy Dispersive Analysis of X-rays), and the results indicated the presence of some sulphate salts. These minerals result from chemical reactions between carbonate cement and the gases O_2 , SO_2 , and CO_2 dissolved into the moisture [14]. In conclusion, research on salt degradation has primarily concentrated on immovable outdoor cultural heritage [15], with less research on cultural heritage preserved in an underground environment.

In 2014, during the construction of the Chuanshi vehicle section of Line 7 of the Chengdu Metro in Sichuan Province, China, a large Ming dynasty burial site was discovered. Sichuan Province is located in the southwest of China. The distribution of burials is shown in Figure 1a, and the distribution in Areas B and C is shown in Figure 1b, c. The burial sites have been proven to be the burial ground of the eunuchs of the Shu King in the Ming dynasty. These tombs are all stone constructions and decorated with paintings and carving on the stone surface, with gilding in some areas. These painted stone carvings are of great historical, artistic, and scientific value. Due to the complex and changing environment of the archaeological excavation site, the Chengdu Institute of Cultural Relics and Archaeology decided to relocate the cultural relics to protect them better and display the painted stone carvings. In 2016, after nearly two years of in situ conservation, 23 tombs of higher value in tombs 1 to 19 in Area B and tombs 1 to 4 in Area C were selected for relocation. The painted stone carvings were packed into custom-made wooden boxes containing cushioning material. They were then covered layer-by-layer with rice paper and a soft cloth to insulate the cultural relics from the outside environment. A photograph of the interior of the wooden box is shown in Figure 1d. Then, they were stored in Pujiang Museum in Chengdu, Sichuan. They were sealed and preserved until 2020. In May of 2020, when the tombs were unpacked and inspected, it was found that the painted stone carvings had suffered severe deterioration in the form of paint loss, salt efflorescence, biodeterioration due to microbial proliferation, and punctate loss which means that the paint layer was peeling off in the form of dots. Thus, these painted stone carvings urgently needed conservation and restoration.

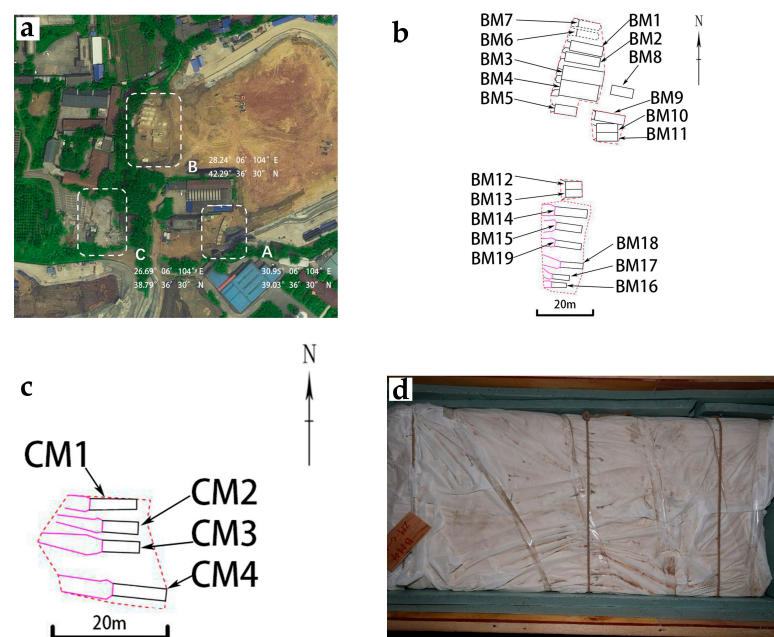


Figure 1. (a) Area of burial distribution; (b) distribution of burials in Area B; (c) distribution of burials in Area C; (d) interior of the wooden box.

In this research, the salt efflorescence of these painted stone carvings was selected as the object of study. To provide a basis for the removal and prevention of the salt efflorescence on these painted stone carvings, the composition of the salt efflorescence, the sources of the crystalline salts, and the damage to the paint layer of the painted stone carvings are investigated.

2. Materials and Methods

2.1. Sample Collection

In order to confirm the specific composition of the salt efflorescence, the samples were taken from cultural relics with extensive paintings and that were severely diseased. Four samples were obtained from the white areas of graves 2 and 4 in Area B on 24 August 2020 in Pujiang Museum's storage room. Graves 2 and 4 in Area B are preserved in the southeast corner of Pujiang Museum's storage room. One sample of the stone substrates was also obtained from grave 2 in Area B. Details of the samples are given in Table 1. The sampling locations are shown in Figure 2.

Table 1. Description and analysis methods of samples collected from the painted stone carvings.

Number	Samples	Analysis Method
1	Pigment fragments with salt efflorescence	OM, RAM, IC
2	Salt powder	IC
3	Salt powder	IC
4	Salt powder	IC
5	Stone substrates fragments	XRF, XRD, PM

"OM" means optical microscopy; "RAM" means micro-Raman spectroscopy; "IC" means ion chromatograph; "XRF" means X-ray fluorescence spectrometer; "XRD" X-ray diffractometer; "PM" means polarized light microscope.

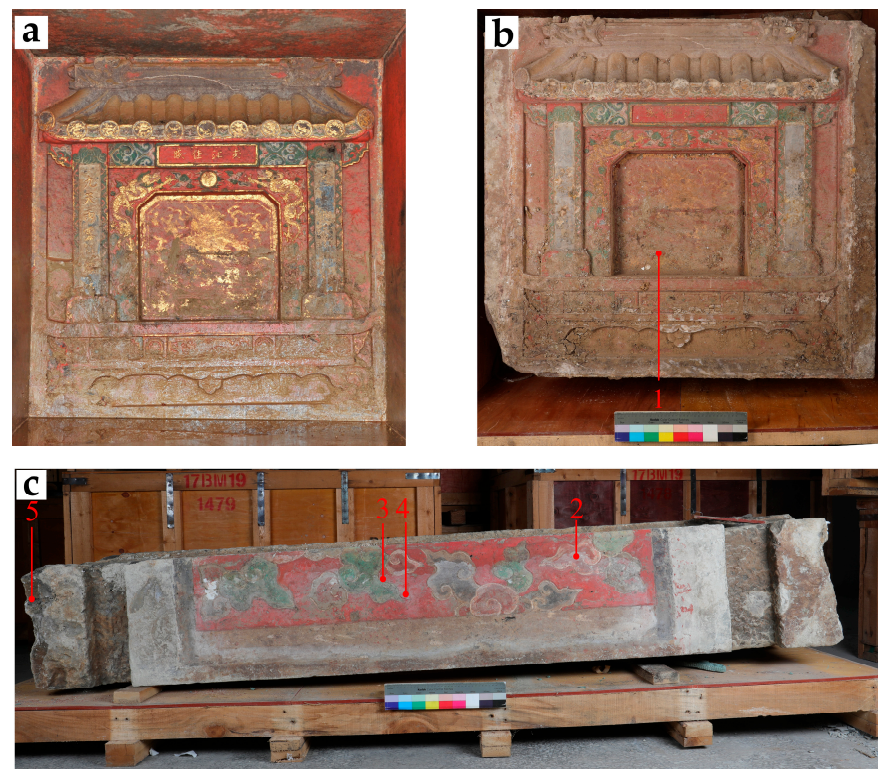


Figure 2. (a) Photograph of the posterior chamber of tomb 4 in Area B at the time of excavation; (b,c) preservation of the painted stone carvings of the posterior chamber of tomb 4 in Area B and tomb 2 in Area B at the time of the inspection in May 2020 and the location of the sampling.

2.2. Instrumentation and Measurements

Optical microscopy (OM): KEYENCE VHX-6000 ultra-depth-of-field 3D video microscope for viewing the surface morphology of the samples. Magnification: 20 to 2000 \times .

Micro-Raman spectroscopy (RAM): HORIBA XploRA fully automatic micro confocal laser Raman spectrometer with 532 nm, 638 nm, and 785 nm lasers, 1200 gr/mm grating, with an Olympus optical microscope. Test using an objective lens of 50–100 \times , a spatial resolution of less than 1 μm , the spectral resolution at 532 nm is 1.8 cm^{-1} and at 785 nm, it is 1.1 cm^{-1} .

Ion Chromatograph (IC): Ion chromatograph using the ion chromatography system model HIC-10A super IC manufactured by Shimadzu, Japan; the component equipment models and parameters are listed in Table 2. The LCsolution Ver. 1.21 sp1 chromatography workstation was used for chromatography system control, data acquisition, and processing. The ion chromatography test conditions are listed in Tables 3 and 4.

Table 2. Shimadzu HIC-10A super IC ion chromatography system equipment parameters.

Equipment	Models and Parameters
High-pressure infusion pumps	LC-10ADsp
Column temperature chamber	CTO-10A
Conductivity detectors	CDD-10Asp
System controllers	SCL-10Asp
In-line vacuum degassers	DGU-12A
Anion separation columns	Shim-pack IC-SA3, column length 250 mm, inner diameter 4.0 mm
Anion separation protection columns	Shim-pack IC-SA3(G), column length 10 mm, inner diameter 4.6 mm
Anion suppressors	SUPPRESSOR CARTRIDGE ANION
Cationic separation columns	Shim-pack IC-SC1, column length 150 mm, inner diameter 4.6 mm
Cationic separation protection columns	Shim-pack IC-SC1(G), column length 10 mm, inner diameter 4.6 mm
Cation suppressors	SUPPRESSOR CARTRIDGE KATION

Table 3. Test conditions for ion chromatography anions.

Mobile Phase	0.35 mmol/L Na ₂ CO ₃ Aqueous Solution
Column temperature	45 °C
Flow rate	0.8 mL/min
Column pressure	11 MPa
Sampling volume	60 μL
Data recording start and end times	0–30 min

Table 4. Test conditions for ion chromatography cations.

Mobile Phase	0.70 mmol/L H ₂ SO ₄ Aqueous Solution
Column temperature	40 °C
Flow rate	1.0 mL/min
Column pressure	5.9 MPa
Sampling volume	60 μL
Data recording start and end times	0–20 min

For the ion chromatograph test, the standard samples of chloride ion (Cl^-), sulphate ion (SO_4^{2-}), sodium ion (Na^+), potassium ion (K^+), magnesium ion (Mg^{2+}), and calcium ion (Ca^{2+}) were all 100 mg/L and purchased from the China National Research Centre for Standard Substances. The sodium carbonate (Na_2CO_3) and sulphury acid (H_2SO_4) were all analytically pure. High-purity water was purchased from Beijing Zhongke Shengze Technology Development Co., Ltd., with a resistance value greater than 18 $\text{M}\Omega\cdot\text{cm}$. A

specific sample and a known mass of high-purity water were prepared into a water solution, sonicated for 15 min, and left to stand for 48 h. The upper layer of the clear solution was filtered using a disposable aqueous needle filter and directly fed into the sample for determination. The disposable aqueous needle filter was purchased from Tianjin AUTO-SCIENCE Instruments Co.

X-ray diffractometer (XRD): Nihon Rei Ultima IV diffractometer. The sample was ground and pressed into a flat surface in the sample bath for testing. Powder crystal determination conditions: Cu target, power: 1.6 kW, scan speed: $20^{\circ}/\text{min}$, and 2θ scan range: $10\text{--}100^{\circ}$.

X-ray fluorescence spectrometer (XRF): Bruker PUMA S2 energy dispersive X-ray fluorescence analyzer. The test conditions were: Ag target, tube voltage 40–50 kV, current 2 mA, and smart mode.

Polarized light microscope (PM): Leica DM2700P polarized light microscope, where rocks are made into thin sections ($22\text{ mm} \times 22\text{ mm}$, 0.3 mm thick) and then observed under single and orthogonal polarization conditions to determine the rock type and characteristics, respectively.

3. Results and Discussion

3.1. Analysis of Salt Efflorescence Composition

3.1.1. Microscopic Observations

In order to clarify the microscopic morphology of the salt efflorescence, sample 1 was placed under an OM. The results show that the salt efflorescence is distinctly granular, mainly on the surface of the red pigment layer, with negligible diffusion in the stone substrates, as shown in Figure 3.

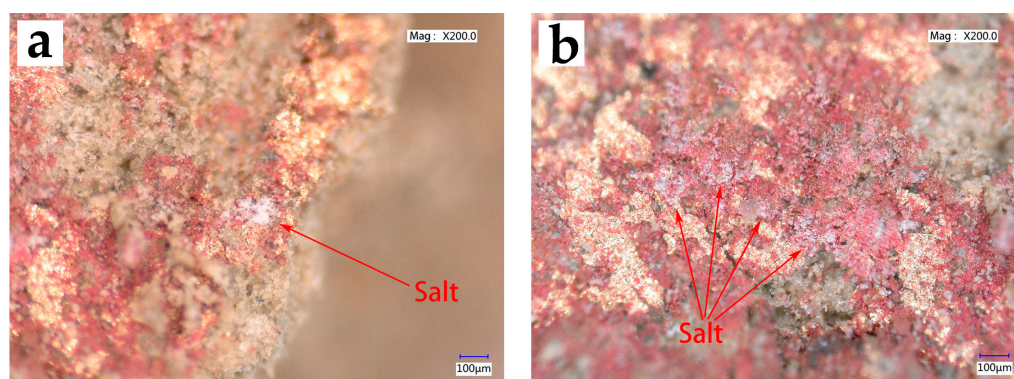


Figure 3. OM image of the salt efflorescence on the surface of sample No. 1. (a,b) are both micrographs of sample No. 1 under the OM.

3.1.2. Raman Analysis

Raman has been used for over 30 years in the study of cultural heritage, with its high spatial resolution, molecular specificity, and ability to perform non-destructive or micro-destructive analysis. It is used to identify minerals, gemstones, organic and inorganic pigments, their degradation products, varnish, plastic, glass, ceramic analysis, and conservation treatments [16].

In order to determine the type of this salt efflorescence, Raman was performed on the salt efflorescence of sample 1. The results show characteristic peaks at 253 cm^{-1} , 342 cm^{-1} , 413 cm^{-1} , 491 cm^{-1} , 616 cm^{-1} , 1008 cm^{-1} , and 1136 cm^{-1} . The characteristic peaks near 413 cm^{-1} , 491 cm^{-1} , 616 cm^{-1} , 1008 cm^{-1} , and 1136 cm^{-1} are similar to the standard peak of gypsum ($\text{CaSO}_4 \cdot 2\text{H}_2\text{O}$) [17]. Moreover, the characteristic peaks at 253 cm^{-1} and 342 cm^{-1} are consistent with the Raman spectrum of cinnabar (HgS) [18], which is presumably the result of laser light passing through the surface layer of salt efflorescence to the underlying red pigment layer. The Raman tested point and characteristic peaks for sample 1 are shown in Figure 4.

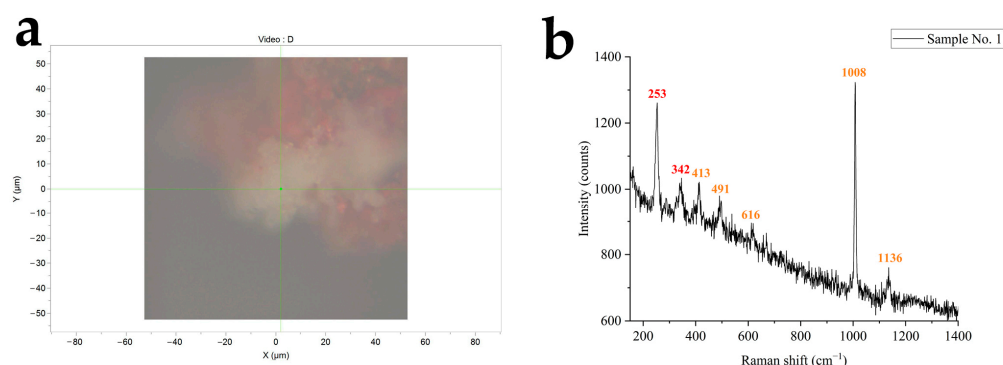


Figure 4. (a) OM image and Raman-tested point of the salt efflorescence in sample No. 1, (b) characteristic peaks for sample No. 1.

3.1.3. IC Analysis

To confirm whether this sample also contained other soluble salts, ion chromatography was carried out on samples 1 to 4, and the results are shown in Table 5. The results showed that the four samples included six ions: Na^+ , NH_4^+ , K^+ , Ca^{2+} , Cl^- , NO_3^- , and SO_4^{2-} . The concentrations of SO_4^{2-} and Ca^{2+} ions were much higher than those of the other ions, and it could be concluded that calcium sulfate was the main component of the crystalline salt, which is compatible with the results of the Raman analysis. Therefore, the majority of the salt efflorescence in these samples consists of gypsum ($\text{CaSO}_4 \cdot 2\text{H}_2\text{O}$), with trace quantities of Na^+ , NH_4^+ , Cl^- and NO_3^- ions.

Table 5. Test results of ion chromatography (mg/g).

No.	Na^+	NH_4^+	K^+	Mg^{2+}	Ca^{2+}	Cl^-	NO_3^-	SO_4^{2-}
1	0.082	0.087	0.050	-	13.267	0.045	-	31.564
2	0.257	0.032	0.064	-	4.653	0.218	-	15.677
3	0.045	0.106	0.087	-	53.521	0.101	-	128.337
4	0.172	0.033	0.025	-	-	0.229	0.690	0.473

“-” means not detected.

Gypsum is a typical salt damage in cultural heritage found in Angkor monuments and Dunhuang Mogao Grottoes [19,20]. Compared to Hanyangling and Mogao Cave 351, the gypsum content in samples 1 to 3 is relatively high, while the remaining Na^+ , NH_4^+ , Cl^- , and NO_3^- ions are similar [19,21], which also indicates a high level of gypsum enrichment on the surface of these painted stone carvings.

3.2. Analysis of the Causes of Salt Efflorescence

The above analysis confirms that the salt efflorescence on the paint layer surface of the painted stone carvings is predominantly composed of gypsum. It is assumed that there are two possible sources for this salt, one being that the stone substrates contain gypsum internally, which migrates to the surface of the paint layer with moisture due to changes in the external environment. After moisture evaporation, gypsum generates a white area on the paint layer's surface. The second possible source of gypsum is the external environment. Along with the groundwater, the salts in the soil around the burial migrated from fissures to the surface of the painted stone carvings. To this end, rock sample 5 was analyzed, and the preserved environment of painted stone carvings was investigated to confirm the source of the gypsum.

3.2.1. XRF Analysis

The XRF analysis of stone sample 5 revealed that the stone substrate is mainly composed of five elements, including Si, Ca, Fe, Al, and K, with Ca accounting for as much as 31.74% of the total. Table 6 displays the XRF results of sample 5. Comparing the XRF results

quartzite, and carbonate rocks, with a grain size of 0.05–0.20 mm. The interstitial filler consists of fines of the same composition that have been mechanically fractured, carbonate minerals, clay minerals, and metallic minerals. The predominant kind of cementation is pore-type cementation. Carbonate minerals are irregular, colorless, their interference color is a high-order whitish-pale, in the form of cementation, unevenly distributed, and the content is about 10–15%. The clay minerals are finely grained, gap-fill distributed, and present in concentrations lower than 5%. The metallic minerals are irregularly grained, black, and non-luminous, 0.02–0.25 mm in size, scattered, and less than 5%. Zircon is occasionally seen in columnar form, colorless, with its interference color in the third order and it has parallel extinction and a grain size of 0.05–0.10 mm. Tourmaline is occasionally seen in prismatic form, uneven color, and green and has yellow-green-light yellow-green pleochroism, interference color second order, parallel extinction, and a grain size of around 0.08 mm. According to the results, the stone sample consists mainly of quartz, feldspar, mica, rock chips, and a cement matrix. The petrographic microstructure of sample 5 is shown in Figure 6.

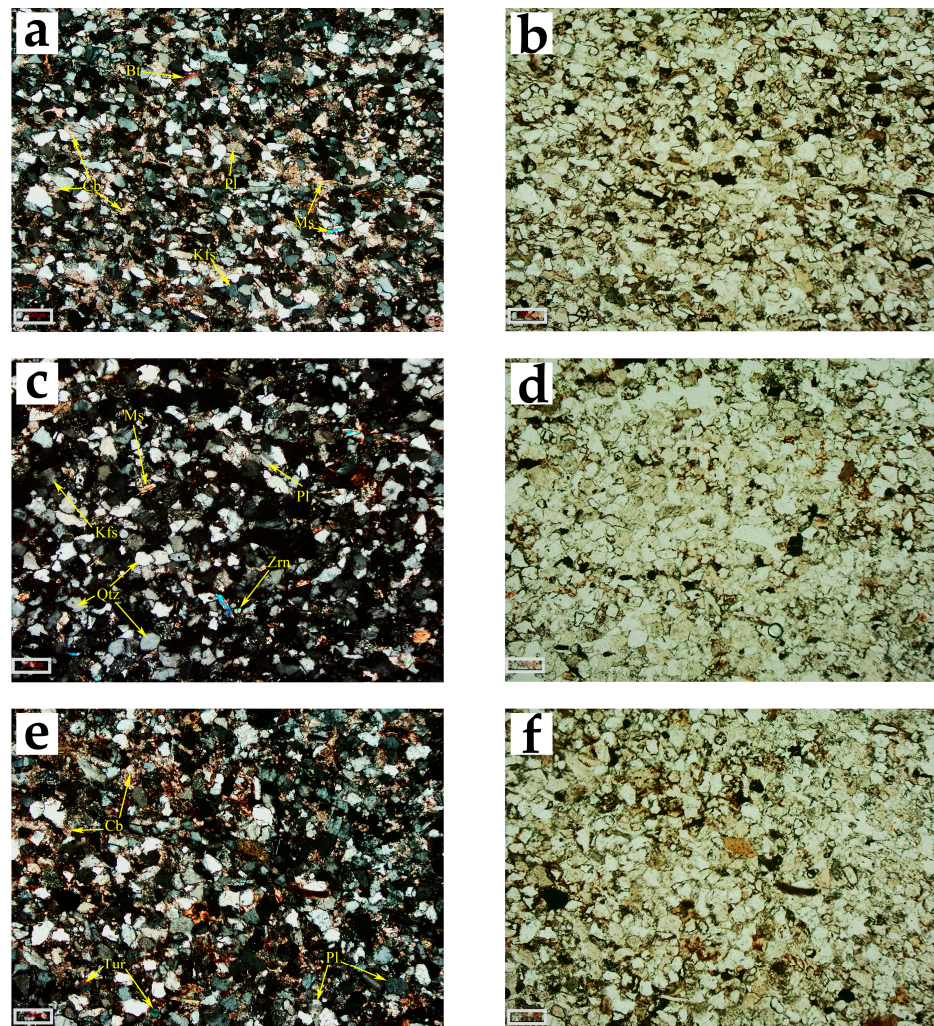


Figure 6. Petrographic microstructure of sample No. 5. (a,c,e) are the petrographic microstructures in the orthogonally polarized view and (b,d,f) are the corresponding single polarized view. “Qtz” means quartz; “Kfs” means K-feldspar; “Pl” means plagioclase; “Bt” means biotite; “Ms” means muscovite; “Cb” means carbonate mineral; “Zrn” means zircon; “Tur” means tourmaline.

The above analysis results indicate that the stone substrates of the painted stone carvings are sandstone. Moreover, the rock contains considerable levels of Ca and the compound is calcite and dolomite, which worked as binding agents of the sandstone [24,25].

Therefore, the gypsum on the surface of the painted stone carvings did not originate from within the stone substrates.

3.2.4. Preservation Environment Survey

China is the third-largest acid rain region in the world, with 40% of its area affected by acid rain [26]. These painted stone carvings were excavated in Jinjiang District, Chengdu, Sichuan Province, and the Sichuan Basin is a high-incidence area for acid rain in China. From 2006 to 2013, Zhao et al. analysed the characteristics of acid rain changes in Sichuan. They showed that the probability of acid rain in Chengdu was 61.5% and the pH value was 4.28, which was strongly acidic [27]. Zhang Yanmei studied PM_{2.5} on hazy days in Chengdu and found that NO_3^- and SO_4^{2-} dominated the anions, while NH_4^+ , Na^+ , and Ca^{2+} dominated the cations [28]. Moreover, the Ming tomb used mortise and tenon joints, with significant spaces between certain stones. Due to the unstable geological substrate, this group of tombs also exhibited structural damage, such as north–south misalignment and general deformation. The construction and state of preservation of the burial chambers are shown in Figure 7.

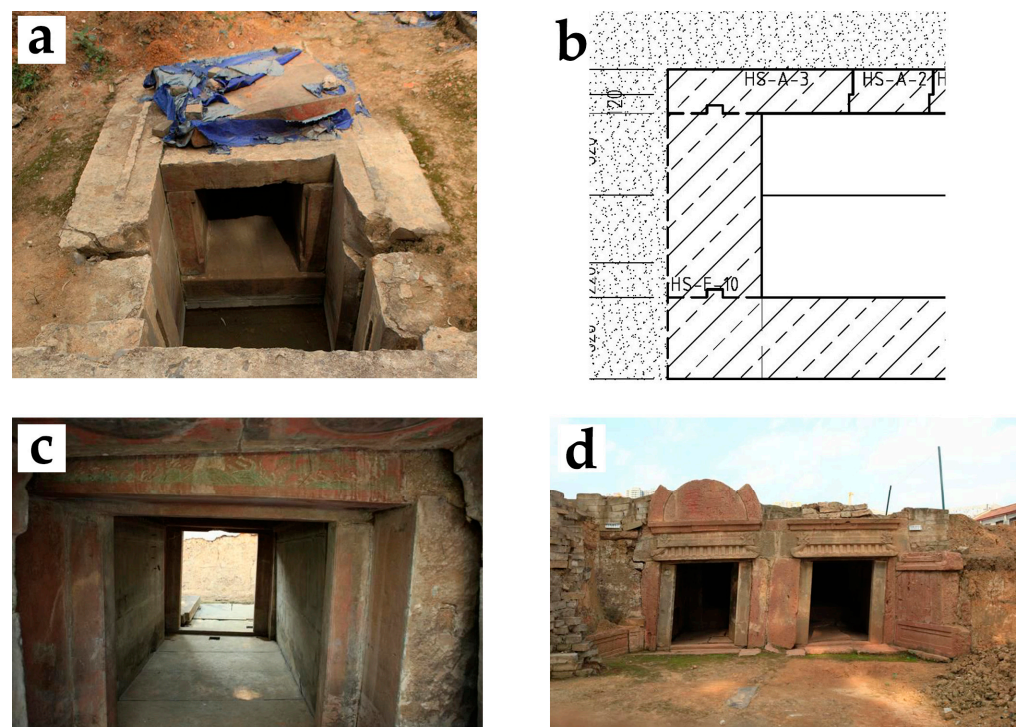


Figure 7. Photos of the construction and state of preservation of the burial chamber. (a,b) is the mortise and tenon joints of the burial chamber and their diagrams; (c) is the misalignment of the burial chamber; and (d) is the deformation of the burial chamber.

The presence of water stains and white material around the fissures of the stone substrates in the burial chambers was found, which is very similar to the salt efflorescence on the painted surfaces, as shown in Figure 8. In Chengdu, where acid rain is frequent, large quantities of SO_4^{2-} ions combine with acid rain or Ca^{2+} ions in the soil to form gypsum. Gui Dan analyzed the burial soil in the Chengdu area, and the results showed that the content of Ca^{2+} , Na^+ , SO_4^{2-} , and NO_3^- ions were high, which is consistent with the above inference [29]. The gypsum gradually migrates with the groundwater along the fissures of the burial chamber to form water stains. When the water evaporates or becomes supersaturated, white areas will form on the surface of the burial chamber walls.

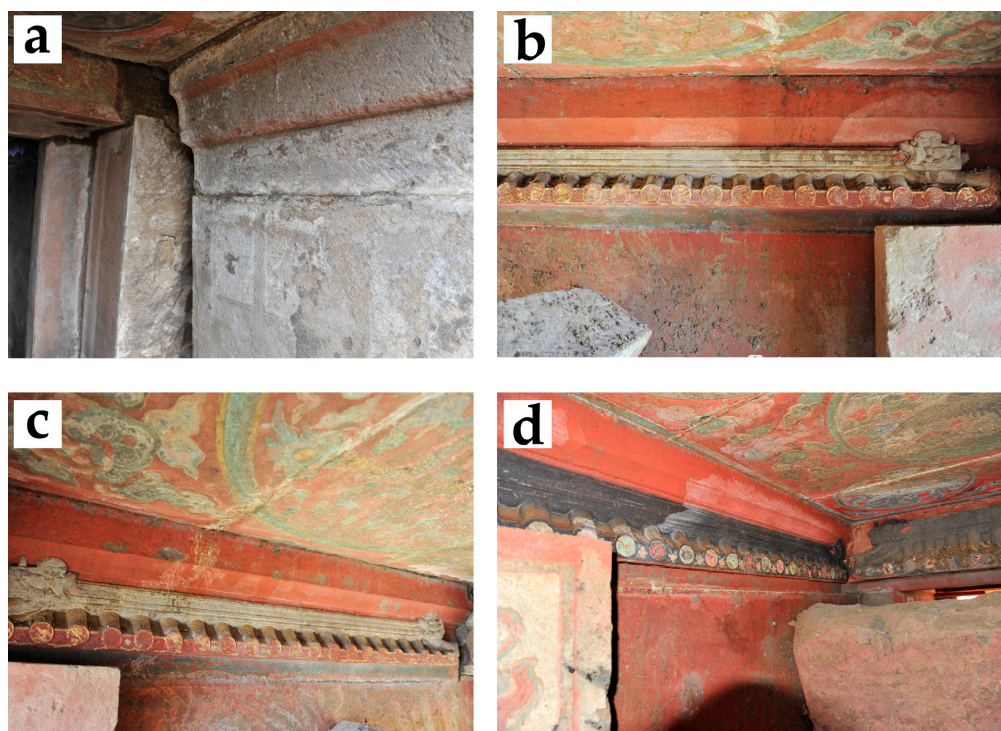


Figure 8. Water stains and white material in the burial chamber at the excavation site. (a) Area B, tomb 1; (b,c) Area B, tomb 3; (d) Area B, tomb 4.

After being packed into a wooden box in 2016, the painted stone carvings were relocated to Pujiang Museum in Chengdu for sealed storage. Therefore, salt efflorescence should be relatively stable during this stage, and no ionic exchange occurs with the outside world. In conclusion, the salt efflorescence on the surface of the painted stone carvings was formed during the burial process and resulted from a combination of acid rain, soil, and groundwater.

3.3. Analysis of Salt Efflorescence Hazards

Based on the identification of the salt efflorescence and the initial identification of the source of the salt efflorescence, the following section analyzes the influence of gypsum on the paint layer. According to the previous experimental analysis and the preservation environment survey of the painted stone carvings, it was judged that the damage caused by calcium sulphate in this study was primarily physical, including crystallization pressure and hydration pressure [30]. It has been shown that when $C/C_s = 2$ (C/C_s is the degree of supersaturation, where C is the existing solute concentration and C_s is the saturation concentration), the crystallization pressure of CaSO_4 at $8\text{ }^\circ\text{C}$ is 33.5 MPa and that of $\text{CaSO}_4 \cdot 2\text{H}_2\text{O}$ is 28.2 MPa [31]. In addition, the higher the relative humidity at a constant temperature, the higher the hydration pressure for conversion of $\text{CaSO}_4 \cdot 0.5\text{H}_2\text{O}$ to $\text{CaSO}_4 \cdot 2\text{H}_2\text{O}$, up to 219 MPa within $0\text{--}20\text{ }^\circ\text{C}$ [32]. Charola's research concluded that the deterioration of buildings and monuments by gypsum is the result of the crystallization cycles of this salt. Although gypsum can dehydrate to a hemihydrate (bassanite) and an anhydrate (anhydrite), in nature, this reaction occurs slowly, sometimes on a geological time scale and, therefore, it is unlikely to occur when gypsum is found on and in building materials. Thus, the gypsum deterioration in building stones cannot be attributed to hydration pressures. As with other non-hydrating salts, it results from its crystallization pressure within the porous material [33]. Therefore, in these painted stone carvings, the destruction caused by gypsum is mainly caused by crystallization pressure.

The preservation process of these stone carvings can be divided into three stages. Firstly, before excavation, although there were some fissures in the chamber environment of

the painted stone carvings, the overall preservation environment was still relatively closed, and its relative humidity was maintained at a high value. During this process, calcium sulphate is continuously produced. It adheres to the paint layer's voids, which are gradually damaged by water penetration, high humidity, and changes in ionic concentration. The second stage is during the in situ preservation period; in this stage, the most frequent changes in temperature and humidity occur. Although the tomb was briefly protected after excavation, the original closed environment of the tomb was broken during excavation. Moreover, the external environment significantly affected the internal temperature and humidity, so the salt damage in the second stage should be the most intense. The third stage is the storage of the painted stone carvings in Pujiang Museum, where they have been kept in sealed wooden boxes and are less affected by fluctuations in the external environment, so gypsum should be the most stable in this stage.

The presence of salts is one of the leading causes of deterioration of art objects with a porous nature, particularly wall paintings and stone statues. Crystallizing salts may be locally concentrated as efflorescence on the artwork surface or as less apparent but much more damaging sub-efflorescence in the subsurface of the porous materials. Cyclic solubilization and crystallization takes place with fluctuating environmental conditions, inducing mechanical stress in the pores and flaking of the artistic surface [34,35]. In order to assess the extent of salt damage affecting the painted stone carvings, the area of salt efflorescence and paint layer diseases (including both paint loss and punctate loss) in tombs 2, 3, 4, and 9 in Area B were counted. Table 7 displays the detailed data. Comparing the salt efflorescence area with the paint layer disease area in the four tombs mentioned above, it is evident that the paint layer disease area in the other three tombs, except for tomb 2, increases with the salt efflorescence area which also reflects salt efflorescence's role in promoting the production of paint layer diseases in painted stone carvings.

Table 7. Area statistics of salt efflorescence and paint layer diseases in tombs 2, 3, 4, and 9 in Area B.

Burial Number	BM2	BM3	BM4	BM9
Area of salt efflorescence/m ²	2.32	0.34	4.11	2.13
Area of paint layer diseases/m ²	1.464	0.91	10.13	3.64

After more than half a century of development, the current protection methods for burial-mural-type cultural relics in China could be divided into two categories: in situ protection and relocation protection. In situ conservation can preserve the historical and cultural information of burial murals to the maximum extent. However, because of the complex and variable preservation environment after excavation, there are not many burial murals that can be conserved in situ and open to the public [36,37]. Relocation protection refers to the relocation of the entire tomb for better protection; this method is better for preserving tomb information. Nevertheless, the cost demand is higher. In recent years, with China's rapid economic development and increasing attention to cultural relics' conservation, the number of relocation conservation cases has increased for burial murals with high value, a poor preservation environment, or a significant impact on capital construction projects. The painted stone carvings in this research had taken the approach of relocating the whole group for conservation. Before the relocation, the preservation of these cultural relics and the disease area were recorded in detail, which laid a solid foundation for the follow-up work. However, there is still a lack of environmental monitoring data during in situ preservation, creating some difficulties for subsequent analysis of disease causes. Overall, the relocation to Pujiang museum for preservation has greatly limited the development of crystalline salt disease, providing favourable conditions for conserving cultural relics. Thus, for the same type of heritage conservation, controlling the environment is the primary way to prevent weathering.

4. Conclusions

The analysis of the white substance on the painted stone carvings' surface at Pujiang Museum by various analytical methods, including OM, RAM, and IC, indicates that the white substance is salt efflorescence, with $\text{CaSO}_4 \cdot 2\text{H}_2\text{O}$ as the main component.

Analysis of samples from the stone substratum proved that the stone did not contain gypsum internally. Environmental surveys show that acid rain is frequent in the Chengdu area, and the photographs of the excavation site also show numerous gaps between the stone substrates. Therefore, gypsum results from the combined effect of acid rain, soil, and groundwater during the long-term burial process.

The crystallization pressure of calcium sulphate is relatively high, and its damage to the paint layer of painted stone carvings can be divided into two stages. Firstly, the preservation environment is relatively stable in the chamber before excavation. However, calcium sulfate will also damage the paint layer due to the influence of water seepage and a high humidity environment and ionic concentration. The second stage is after excavation and before relocation. At this stage, the temperature and humidity change frequently, and the damage to gypsum in the paint layer should be more intense.

Author Contributions: Conceptualization, Q.S., J.Z. and Y.B.; methodology, H.G., Q.S. and J.Z.; investigation, H.G., Q.S. and L.C.; data curation, Q.S. and J.Z.; writing—original draft preparation, Q.S.; writing—review and editing, J.Z., H.G. and Y.Z.; supervision, H.G. All authors have read and agreed to the published version of the manuscript.

Funding: This research was financially supported by the National Key R&D Program of China (grant number 2020YFC1522404).

Data Availability Statement: Not applicable.

Acknowledgments: We thank Wang Ning, Yang Tao, and Chen Juncheng for their support and guidance during the sampling process; we also thank Hu Fengdan, Gui Dan, and Zheng Yixuan for their assistance during the experiment.

Conflicts of Interest: The authors declare no conflict of interest.

References

1. Ma, C.L.; Liu, Z.J.; Cheng, L. Raman spectroscopy, X-ray fluorescence and scanning electron microscopy of painted pigments in the Longmen Grottoes. *J. Light Scatt.* **2018**, *30*, 357–361. [[CrossRef](#)]
2. He, X.; Bu, H.; Zhang, N.; Guo, H. Analysis of colour pigments in stone carvings from the Qianfo Cliff Caves, Guangyuan. *Spectrosc. Spectr. Anal.* **2021**, *41*, 967–972.
3. Li, Q.Q.; Yang, Z.K.; Gao, S.; Zhou, L.L.; Wei, S.Y.; Ma, Q.L. An analysis of the stone and vermilion pigments of some Northern Qi Buddhist statues at Longxing Temple, Qingzhou, Shandong. *Sci. Conserv. Archaeol.* **2017**, *29*, 55–62. [[CrossRef](#)]
4. Zhang, Y.J.; Wu, H.; Liang, J.F.; Zhao, X.C.; Zhao, J. Conservation and restoration of excavated Buddhist statues from Dayun Temple, Jingchuan, Gansu. *Relics Mus.* **2018**, *204*, 90–95.
5. Sablier, M.; Garrigues, P. Cultural Heritage and Its Environment: An Issue of Interest for Environmental Science and Pollution Research. *Environ. Sci. Pollut. Res.* **2014**, *21*, 5769–5773. [[CrossRef](#)]
6. Li, Z. *Conservation of the Silk Road Cave Murals*; Science Press: Beijing, China, 2005.
7. Zhang, L.S.; Chen, J.C.; He, S.Y. A review of salt damage mechanisms and suppression studies at soil sites. *Dunhuang Res.* **2020**, *181*, 129–136. [[CrossRef](#)]
8. Guo, H.; Li, M.X.; Song, D.K.; Qiu, Y.X.; Xu, C.C.; Tang, J.Y.; Yang, F.J. A study of the mechanism of alkali damage to the murals of the Mogao Caves at Dunhuang I. *Dunhuang Res.* **1998**, 153–163+188.
9. Guo, H.; Li, M.X.; Qiu, Y.X.; Xu, C.C.; Tang, J.Y.; Yang, F.J. A study of the mechanism of alkali damage to the murals of the Mogao Caves at Dunhuang II. *Dunhuang Res.* **1998**, 159–172+184.
10. Guo, H.; Li, M.X.; Qiu, Y.X.; Xu, C.C.; Tang, J.Y.; Yang, F.J. A study of the mechanism of alkali damage to the murals of the Mogao Caves at Dunhuang III. *Dunhuang Res.* **1999**, 153–175.
11. Dei, L.; Mauro, M.; Bitossi, G. Characterisation of Salt Efflorescences in Cultural Heritage Conservation by Thermal Analysis. *Thermochim. Acta* **1998**, *317*, 133–140. [[CrossRef](#)]
12. Flatt, R.J. Salt Damage in Porous Materials: How High Supersaturations Are Generated. *J. Cryst. Growth* **2002**, *242*, 435–454. [[CrossRef](#)]
13. Siedel, H. Salt Efflorescence as Indicator for Sources of Damaging Salts on Historic Buildings and Monuments: A Statistical Approach. *Environ. Earth Sci.* **2018**, *77*, 572. [[CrossRef](#)]

14. Liu, R.Z.; Zhang, B.J.; Zhang, H.; Shi, M.F. Deterioration of Yungang Grottoes: Diagnosis and Research. *J. Cult. Herit.* **2011**, *12*, 494–499. [[CrossRef](#)]
15. Delgado, J.M.P.Q.; Guimarães, A.S.; de Freitas, V.P.; Antepará, I.; Kočí, V.; Černý, R. Salt Damage and Rising Damp Treatment in Building Structures. *Adv. Mater. Sci. Eng.* **2016**, *2016*, e1280894. [[CrossRef](#)]
16. Casadio, F.; Daher, C.; Bellot-Gurlet, L. Raman Spectroscopy of Cultural Heritage Materials: Overview of Applications and New Frontiers in Instrumentation, Sampling Modalities, and Data Processing. *Top. Curr. Chem. (Z)* **2016**, *374*, 1–51. [[CrossRef](#)] [[PubMed](#)]
17. Sarma, L.P.; Prasad, P.S.R.; Ravikumar, N. Raman Spectroscopic Study of Phase Transitions in Natural Gypsum. *J. Raman Spectrosc.* **1998**, *29*, 851–856. [[CrossRef](#)]
18. Burgio, L.; Clark, R.J.H. Library of FT-Raman Spectra of Pigments, Minerals, Pigment Media and Varnishes, and Supplement to Existing Library of Raman Spectra of Pigments with Visible Excitation. *Spectrochim. Acta Part A Mol. Biomol. Spectrosc.* **2001**, *57*, 1491–1521. [[CrossRef](#)]
19. Chen, G. Study on Salting Damage Analysis and Treatment of Wall Paintings at Mogao Grottoes, Dunhuang. Ph.D. Thesis, Lanzhou University, Lanzhou, China, 2016.
20. Uchida, E. Deterioration of Stone Materials in the Angkor Monuments, Cambodia. *Eng. Geol.* **1999**, *55*, 101–112. [[CrossRef](#)]
21. Wang, Y.J.; Zhou, W.Q.; Dang, X.J.; Wang, Z.; Wang, C. An investigation of the causes of calcium sulfate (CaSO₄·2H₂O) formation on the surface of the underground museum site of Hanyangling. *Sci. Conserv. Archaeol.* **2016**, *28*, 26–30. [[CrossRef](#)]
22. Lu, H.; Fu, W.L.; Chai, J.; Liu, S.; Sun, Z.Y. Analysis of the sandstone of Leshan Giant Buddha based on handheld X-fluorescence spectrometer. *Spectrosc. Spectr. Anal.* **2022**, *42*, 2506–2512.
23. Yan, S.J.; He, K.; Sun, P.; Dou, Y.; Chen, J.Q. Experimental study on the weathering of sandstone at the fishing City ancient battlefield site in Hechuan, Chongqing. *J. Yangtze River Sci. Res. Inst.* **2016**, *33*, 100–104.
24. Morillas, H.; García-Galan, J.; Maguregui, M.; Marcaida, I.; García-Florentino, C.; Carrero, J.A.; Madariaga, J.M. Assessment of Marine and Urban-Industrial Environments Influence on Built Heritage Sandstone Using X-ray Fluorescence Spectroscopy and Complementary Techniques. *Spectrochim. Acta Part B At. Spectrosc.* **2016**, *123*, 76–88. [[CrossRef](#)]
25. Qi, Y.; Wang, M.; Zheng, W.; Li, D. Calcite Cements in Burrows and Their Influence on Reservoir Property of the Donghe Sandstone, Tarim Basin, China. *J. Earth Sci.* **2012**, *23*, 129–141. [[CrossRef](#)]
26. Jiang, X. A Study on the Spatial and Temporal Variability of Soil pH and Its Influencing Factors in the Core Area of Chengdu Plain. Master's Thesis, Sichuan Agricultural University, Ya'an, China, 2018.
27. Zhao, X.L.; Yan, J.; Chen, C.Y.; Huang, X.L.; Guo, X.; Sun, Y. Characterization of acid rain variability in Sichuan from 2006 to 2013. *Meteorol. Environ. Sci.* **2015**, *38*, 54–59. [[CrossRef](#)]
28. Zhang, Y. Research on PM (2.5) Pollution Characteristics of Urban Haze Days in Southwest Acid Rain Area. Master's Thesis, Guizhou University, Guiyang, China, 2016.
29. Gui, D. Reinforcement and Cleaning Research on the Surface Painting of Porcelain Excavated from the Liaojiashan Cemetery in Chengdu. Master's Thesis, University of Science and Technology Beijing, Beijing, China, 2022.
30. Rodríguez-Navarro, C.; Doehne, E. Salt Weathering: Influence of Evaporation Rate, Supersaturation and Crystallization Pattern. *Earth Surf. Process. Landf.* **1999**, *24*, 191–209. [[CrossRef](#)]
31. Winkler, E.M.; Singer, P.C. Crystallization Pressure of Salts in Stone and Concrete. *Geol. Soc. Am. Bull.* **1972**, *83*, 3509. [[CrossRef](#)]
32. Winkler, E.M.; Wilhelm, E.J. Salt Burst by Hydration Pressures in Architectural Stone in Urban Atmosphere. *Geol. Soc. Am. Bull.* **1970**, *81*, 567. [[CrossRef](#)]
33. Charola, A.E.; Pühringer, J.; Steiger, M. Gypsum: A Review of Its Role in the Deterioration of Building Materials. *Environ. Geol.* **2007**, *52*, 339–352. [[CrossRef](#)]
34. Hradil, D. Wall Painting Damage by Salts: Causes and Mechanisms. *Acta Res. Rep.* **2009**, *18*, 27–31.
35. Baglioni, P.; Giorgi, R.; Chelazzi, D. The Degradation of Wall Paintings and Stone: Specific Ion Effects. *Curr. Opin. Colloid Interface Sci.* **2016**, *23*, 66–71. [[CrossRef](#)]
36. Li, M. A discussion of several methods for the conservation of burial murals. *China Cult. Herit. Sci. Res.* **2017**, *48*, 63–72.
37. Yang, W.Z.; Guo, H. Conservation methods of tomb murals in China. *Sci. Conserv. Archaeol.* **2017**, *29*, 109–114. [[CrossRef](#)]

Disclaimer/Publisher's Note: The statements, opinions and data contained in all publications are solely those of the individual author(s) and contributor(s) and not of MDPI and/or the editor(s). MDPI and/or the editor(s) disclaim responsibility for any injury to people or property resulting from any ideas, methods, instructions or products referred to in the content.